Journal of Alloys and Compounds 885 (2021) 160956

Contents lists available at ScienceDirect

Journal of Alloys and Compounds

journal homepage: www.elsevier.com/locate/jalcom

Partial or complete suppression of hysteresis in hydride formation in binary alloys of Pd with other metals

Mikhail Mamatkulov[a], Vladimir P. Zhdanov[a,b,*]

[a] Boreskov Institute of Catalysis, Russian Academy of Sciences, Novosibirsk, Russia
[b] Department of Physics, Chalmers University of Technology, Göteborg, Sweden

ARTICLE INFO

Article history:
Received 2 May 2021
Received in revised form 19 June 2021
Accepted 22 June 2021
Available online 25 June 2021

Keywords:
Palladium
Binary alloys
Hydride
First-order phase transitions
Absorption isotherms

ABSTRACT

At temperatures below 600 K, the isotherms of hydrogen absorption by Pd exhibit hysteresis loops related to the first-order phase transition or, more specifically, to separation of a diluted phase and hydride. According to the experiments, addition of even small amount of the second metal, e.g. Au or Ta, can appreciably suppress hysteresis. This interesting effect is important in various applications, e.g., in the context of fabrication of efficient hydrogen sensors. To clarify its physical background, we present statistical calculations of the hydrogen absorption isotherms for a series of binary alloys of Pd with Mg, Cu, Ag, Ta, Pt, or Au by using the values of the H-metal interaction provided by the density functional theory (DFT). Aiming at the situations with small amount (≤15%) of the second metal, the metal atoms in an alloy are considered to be located at random or with short-range correlations. In the random alloy approximation, appreciable suppression of hysteresis is predicted for all the additives under consideration except Cu. Concerning the correlations, we show that the tendency of metals to mixing (as, e.g., predicted for the Pd–Au or Pd–Ta alloy) is in favour of additional suppression of hysteresis whereas the tendency to segregation (as, e.g., predicted for the Pd-Ag alloy) makes the hysteresis loops wider. For Au and Ta, our findings are in good agreement with available experimental data.

1. Introduction

Beside basic physics and chemistry [1], hydrogen absorption by binary alloys of Pd with other metals is of high current interest in the context of various applications related first of all to the so-called hydrogen economy [2], including hydrogen storage [3–5] and sensors [6–8], and heterogeneous catalysis [9–11]. The specifics of such alloys is that hydrogen absorption in pure Pd is usually more favourable than in other metals and exhibits separation of dilute and dense H phases representing, respectively, a lattice gas and hydride, and accordingly the addition of the second metal to Pd is expected to suppress the absorption itself and the corresponding phase transition to some extent or completely. The observation of all these effects is possible in relatively large NPs or thick supported nanofilms where the hydrogen uptake is determined primarily by absorption in the bulk (the contribution of adsorption at surfaces to the total uptake is negligible in these cases despite larger hydrogen binding energy there). The experiments performed with the Pd–Au and Pd–Cu alloyed nanoparticles (NPs) or, more specifically, nanodiscs with ~ 200 nm diameter and ~ 25 nm thickness at $T \geq 300$ K indicate that the suppression of phase separation can be appreciable even for small fraction, f, of the second metal [12,13]. In particular, the phase-separation-related hysteresis loops in the absorption isotherms are observed at smaller uptakes and become much narrower, and the corresponding critical temperature, T_c, for the phase separation drops from $\simeq$ 600 K in pure Pd to $\simeq$ 300 K in the alloys with Au and Cu already at $f \simeq 0.15$ and $\simeq 0.25$, respectively. Similar effects were earlier observed in Pd-Ni and Pd-Ta films with thickness from 5 to 400 nm and 60 nm, respectively [16,17] and, more recently, in Pd–Co nanohole arrays [18]. The suppression of a hysteresis at low values of f in such binary alloys of Pd is useful in the context of hydrogen sensors [7,14,15]. The requirements (imposed e.g. by U.S. Department of Energy) for such sensors are tough and have not been fully satisfied yet (see e.g. Sec. 1 in Supplementary Information in Ref. [14]), and the Pd-containing nano-alloys are now widely considered to be perhaps the best candidates here.

The very fact of the suppression of the phase transition under consideration due to the presence of the second metal which is a non- or very-weak-hydride former is in principle not surprising

* Corresponding author at: Boreskov Institute of Catalysis, Russian Academy of Sciences, Novosibirsk, Russia.
E-mail address: zhdanov@catalysis.ru (V.P. Zhdanov).

https://doi.org/10.1016/j.jallcom.2021.160956
0925-8388/

because adding it to Pd should increase the energy of absorption at the interstitial sites containing the second metal. It results in the energetic heterogeneity of the absorption sites and can eliminate the phase transition (in statistical physics, the corresponding general models, including e.g. the random-field Ising model, have been studied a few decades since the generic report by Imry and Ma [19]; the phenomenological models focused on hydrogen absorption by Pd alloys are available as well [20,21]). The specific values of f needed for the suppression could, however, hardly be predicted without experiments, and it was/is not clear whether this aspect can be clarified by using first-principles calculations. From the perspectives of the theory, this problem is challenging because the H-metal interaction is relatively weak. In our previous recent study [22] performed in the spirit of ab initio thermodynamics and first-principles microkinetics [23,24] and oriented to large NPs or supported nanofilms where the hydrogen uptake is determined primarily by the bulk, we have shown that in the case of Au the drop of T_c manifested in the suppression of the hysteresis loop in hydrogen absorption isotherms can be quantitatively explained by calculating these isotherms with the parameter values provided by DFT. With suitable validation, the atoms in the alloy were considered to be located at random. More recently, the H/Pd/Au system has theoretically been studied at various f by combining Monte Carlo (MC) simulations and alloy cluster expansion fitted to DFT [25]. Despite different techniques and approximations, the conclusions drown in Refs. [22,25] are similar.

The DFT-based explanation (Refs. [22,25]) of the experimental results obtained for the Pd-Au alloy is far from trivial and might be expected to be occasional (i.e., to hold only in this case) because the H-Au interaction is fairly small, 0.15 eV (see Table 2 or 3 below). From this and other perspectives, it is instructive to clarify by employing DFT what happens in alloys of Pd with other metals. During the past decade, such calculations performed for catalytic reactions occurring on a series of metals were demonstrated to be impactful (see, e.g., the studies by Nørskov and co-workers [26,27]). Following this line, we present here DFT-based calculations of isotherms of hydrogen absorption by binary alloys of Pd with Mg, Cu, Ag, Ta, Pt, and Au. The results for Mg, Cu, Ag, Ta, and Pt are novel. As in Ref. [22], the focus is on the effect of addition of the second mental on the corresponding first-order phase transition. Also as in Ref. [22], f is considered to be low because, as already noticed, this limit is of practical importance from the perspective of sensors and what happens in this case is not clear. Some of the details (e.g., the cutoff energy) of our present DFT calculations are slightly different compared to those used earlier [22] for the Pd-Au alloy. In fact, however, the earlier and present results for this alloy are nearly identical. The statistical analysis is done assuming the metal atoms to be located at random or with short-range correlations.

Concerning the use of DFT in the context under consideration or similar contexts, we can add that the DFT studies focused on hydrogen absorption by metals are now numerous (briefly reviewed in [22]; for Pd and Pd hydride, see e.g. a recent review by Setayandeh et al. [28]). Referring to more recent studies, we may notice that Setayandeh et al. [29,30] have articulated the challenge of accurate description of electron and phonon band structures of the Pd hydrides including PdH and Pd_3VacH_4 (the superabundant vacancy phase) [28]. Borgschulte et al. [31] have analyzed vibrational frequencies in the hydride (ZrV_2H_2) where the distance between nearest-neighbour H atoms is appreciable shorter than in the conventional hydrides. Chen and Mavrikakis [32] have studied hydrogen absorption by small PdPt nanoclusters. Chen et al. [33] have calculated hydrogen solubility in Pd_3Ag. Zhou and Curtin [34] have scrutinized H absorption, surface, and fracture energies in the case of stainless steel, CoCrFeNi, and CoCrFeMnNi. In the context of high-temperature superconductivity, Troyan et al. [35] have described yttrium hexahydride by using "superconducting" DFT. In our context, we note that the results reported in all these studies are either not directly applicable or not sufficient for calculations of the hysteresis-containing isotherms of hydrogen absorption in the Pd-based binary alloys.

Our presentation below is divided into four parts focused on the computational methods (Sec. 2), results and discussion (Sec. 3), conclusions (Sec. 4), and Bethe-Peierls approximation allowing us to take short-range correlations into account (Appendix).

2. Computational methods

2.1. Statistics

The specifics of absorption of hydrogen in binary alloys of Pd with other metals is determined by the type of arrangement of metal atoms in an alloy, energies of the interaction of hydrogen atoms with metal atoms, and hydrogen-hydrogen (H–H) interaction. The arrangement of metal atoms depends on f, details of the metal-metal interactions, and on the way and conditions of the alloy fabrication and use and in general may be very diverse [36]. The H-metal and H-H interactions depend on various factors and are complex. Our analysis will be focused on relatively large Pd–M NPs (M is the second metal), e.g., nanodiscs (with ~ 200 nm diameter and ~ 25 nm thickness and $f < 0.2$) fabricated by hole-mask colloidal lithography (as, e.g., in the already mentioned experiments [12,13]). In applications, such NPs are customarily not annealed at high temperatures, and the arrangement of metal atoms is there usually close to random [12,13], and the contribution of the boundary sites to the hydrogen uptake is negligible (in relatively small NPs used in catalysis, the situation is often opposite due to annealing and more important relative role of the surface and subsurface regions; in particular, the sites at the surface play the central role). The absorption at the grain-boundary and dislocation sites is neglected as well in order to simplify the analysis.

In Pd, hydrogen is located primarily in octahedral (O) sites of the fcc lattice (Fig. 1). For the alloys of interest with relatively small f, the hydrogen can be considered to be located in such sites as well. Focusing on hydrogen absorption by these sites, we use the corresponding lattice-gas model. In this model, the energy of interaction of a hydrogen atom with metal atoms depends on the number, n, of M atoms forming a site and their arrangement. For relatively small f, the main contribution to the absorption isotherms is related to the configurations with small n. Our DFT calculations indicate (see below) that in this case the increment of the absorption energy of a hydrogen atom (compared to that in pure Pd) can be considered to depend linearly on n,

$$\Delta E_{\rm abs}(n) = \epsilon_{\rm HM} n, \tag{1}$$

where $\epsilon_{\rm HM}$ is the value corresponding to $n = 1$. Our earlier detailed DFT calculations, performed for the Pd–Au alloy with n up to 6 and the corresponding calculations of the absorption isotherms [22], showed that despite some deviations this linear approximation can

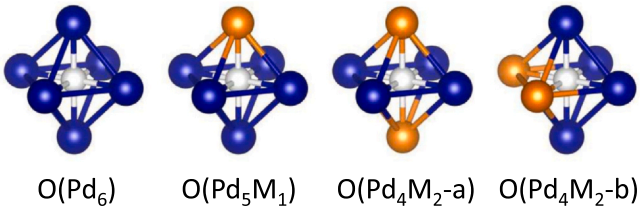

Fig. 1. Unrelaxed O sites for hydrogen absorption in a binary alloy of Pd with the second metal, M. The four structures correspond to the site containing only Pd atoms or Pd atoms with one or two M atoms. Blue (bright gray) and yellow (dark gray) balls correspond to Pd and M atoms, respectively. An H atom is shown by a small white ball in the center of each site.

be used in fact up to $n = 6$. One of the reasons is that we are interested in relatively low values of f, and in this case the contribution of the sites with $n > 2$ to the absorption isotherms is nearly negligible, and accordingly the details of how the energetics of hydrogen absorption by such sites are described are of minor importance.

The addition of the second metal to Pd induces global expansion or contraction of the lattice. This effect results in the downward or upward shift of hydrogen absorption isotherms. Its influence on the shape of isotherms is expected to be negligible and can be ignored in our context [22].

The phase separation observed in Pd or alloys of Pd with other metal is related to the attractive part of the H-H interaction. This interaction, ϵ_{HH}, depends on f. For relatively small f, this effect is weak and its influence on the absorption isotherms is expected to be weaker compared to that of $\Delta E_{abs}(n)$ and accordingly can be neglected [22]. Accepting this approximation, we consider that in the case of alloys ϵ_{HH} is the same as in pure Pd. Accurate calculation of ϵ_{HH} from the first principles is still challenging, because this interaction including the elastic contribution (for this contribution, see e.g. Ref. [37]) is weak and not reduced to the nearest-neighbour one. In our calculations, we use the phenomenological expression including the attractive and repulsive parts,

$$\epsilon_{HH} = -A\theta + \beta A\theta^3, \tag{2}$$

where θ is the H uptake per metal atom or O site, and $A = 0.32$ eV and $\beta = 0.8$ are the corresponding parameters [22]. The conventional attractive (negative) part describes an additive part of the interaction and results in phase separation. The repulsive (positive) part (i) takes into account that at appreciable uptake the interaction becomes strongly non-additive and (ii) reduces adsorption at $\theta > 0.66$.

With the specification above (in particular, neglecting the boundary sites), the hydrogen absorption isotherms are described as [22]

$$\theta = \sum_{n=0}^{6} P_n\, p_n, \tag{3}$$

where P_n is the probability that the absorption site is formed with participation of n M atoms,

$$p_n = \frac{\exp[(\mu - \epsilon_{HM} n + A\theta - \beta A\theta^3)/k_B T]}{1 + \exp[(\mu - \epsilon_{HM} n + A\theta - \beta A\theta^3)/k_B T]} \tag{4}$$

is the probability that such a site is occupied by an H atom, and $\mu = 0.5 k_B T \ln(P_{H_2}) + \text{const}$ is the chemical potential of H atoms (P_{H_2} is the gas-phase pressure). Using (4), we set the H energy in the Pd bulk ($n = 0$) to zero.

For the random-alloy model, we have

$$P_n = \frac{m! f^n (1-f)^{m-n}}{n!(m-n)!}, \tag{5}$$

where $m = 6$ is the maximum number of Au atoms in a site. To take the short-range correlations into account, we have used the Bethe-Peierls approximation (the corresponding details are described in Appendix).

Eqs. (1)–(4) form a statistical basis for our analysis. The assumptions used to derive them are clear from the presentation. Concerning the conditions of their applicability, we can add that as it has long been recognized (see, e.g., Refs. [38,39]) that the hydride formation in metals may be accompanied by plastic deformations, or, more specifically, by generation of dislocations. The likely role of plastic deformations is sometimes experimentally estimated by scrutinizing the width of the hysteresis loops. Such treatments alone are, however, not sufficient because one should bear in mind that although the hysteresis itself does represent the best manifestation of a first-order phase transition, the thermodynamics provides reliably only the equistability condition whereas the width of the hysteresis loops depends strictly speaking not only on thermodynamics but also on kinetics, and its quantitative interpretation is far from straightforward. One of the ingredients of the kinetics is the conditions of the formation of dislocations. Another one is their manifestation in hysteresis loops. Both these ingredients were recently discussed in detail [40–43]. In particular, the analysis based on the conventional theory of dislocations indicates that their formation is energetically favourable provided the NP size (e.g., thickness of nanodiscs as in the experiments under consideration) is larger than 35 nm [40,41]. This conclusion has been drown provided $T \ll T_c$. We are interested in the situation when T is comparable to T_c. Under such conditions, as correctly noted in Ref. [42], the NP size needed for generation of dislocations should be much larger than 35 nm. In very large NPs or macroscopic samples, dislocations can be generated but after a few cycles, work hardening is expected to entangle the existing dislocation network and blocks their further generation [43]. Taken together, these results strongly suggest that the role of dislocations is far from central, and often, e.g. in our context, they can be neglected as it is explicitly declared in [42,43] and as it has been done in Eqs. (1)–(5).

In the systems under consideration, the first-order phase transition is experimentally associated with the hysteresis in absorption isotherms and can theoretically be described by employing Eqs. (1)–(4) at the level of these isotherms as well, i.e., at the level of equilibrium thermodynamics (this approach is widely used since the development of the van der Waals model for interpretation of gas-liquid phase transitions). The kinetics of hysteresis should of course be theoretically clarified at the level of kinetic equations for or MC simulations of hydrogen absorption and desorption (these processes are mediated by adsorption on and desorption from boundary sites). The latter is, however, beyond our present goals.

2.2. DFT

Our present periodic electronic structure DFT calculations, focused on the Pd-based binary alloys, are similar to those performed earlier for the Pd–Au alloy [22]. In brief, we used Vienna Ab-initio Simulation Package [44,45] with the same parameters as in [22] (including the unit cell with 108 metal atoms) except that the cutoff energy was set to 500 eV and Brillouin zone was sampled with a set of $3 \times 3 \times 3$ k-points. The sufficient accuracy of this set has been confirmed by recalculating some of the data with a set of $6 \times 6 \times 6$ k-points (the resulting changes in the absorption energy were smaller than 0.01 eV), and this conclusion is in agreement with earlier DFT calculations of hydrogen absorption in metals (see, e.g., Refs. [46–48]).

To model the influence of alloying on hydrogen absorption, one or two Pd atoms of one octahedral center in the cell was/were replaced by M (M = Mg, Cu, Ag, Ta, Pt, or Au). For each number and arrangement of M atoms, the size of the unit cells was reoptimized. Upon hydrogen absorption, the size of the unit cell was, however, kept fixed since the related volume changes had negligible effect on absorption energetics as already noticed in Ref. [22]. For each number and arrangement of M atoms in the unit cell, the hydrogen absorption energy was calculated as

$$E_{abs} = E(\text{H in metal}) - E(\text{metal}) - E(H_2)/2,$$

where E(metal) is the total energy of Pd cell with 0–2 atoms replaced by M, E(H in metal) is the energy of this cell with a H atom absorbed inside, and $E(H_2)$ is the energy of a H_2 molecule in the gas phase. In calculations of the zero-point energy (ZPE) corrections, only H atoms were allowed to vibrate, since metal atoms are much heavier and their vibrations have practically no effect on those of hydrogen. These corrections reflect in the harmonic approximation that an H atom is light and accordingly slightly delocalized in an absorption site. At the temperatures under consideration (≥300 K; see the

experiments mentioned in the Introduction), this approximation is fairly accurate and now widely used in the area under consideration. For example, it is able to show that the ZPE contribution is decisive in calculating the stability of hydride phases leading to reproducing the experimental fact that Pd hydride is octahedral while not taking account of ZPE leads to a tetrahedral hydride phase as the most stable one [51]. At much lower temperatures, more complex approximations (e.g., based on the path-integral theory) can be used to describe e.g. quantum tunneling during diffusion of H atoms (this regime dominates below 150 K [46]). The latter is, however, beyond the scope of our present study.

3. Results and discussion

As already declared in the introduction, the main goal of our study is to perform DFT-based calculations of isotherms of hydrogen absorption by binary alloys of Pd with various metals including Mg, Cu, Ag, Ta, Pt, and Au and to clarify how low fraction of the second metal influences the hydride-formation-related phase transition in these alloys. This phase transition is manifested in hysteresis loops, and accordingly we should scrutinize how hysteresis disappears with increasing temperature and/or fraction of the second metal. Following this line, we first present the related DFT results and then show the calculated absorption isotherms.

3.1. DFT calculations

To calculate absorption isotherms, we need the H–M interaction, ϵ_{HM}. To determine this interaction, we first calculated the absorption energy of an H atom in an O site of pure bulk Pd [structure O(Pd_6) in Fig. 1]. Then, the absorption energy of an H atom was calculated by replacing one or two Pd atoms of an O site in bulk Pd by, respectively, one or two M atoms [structure O(Pd_5M), O(Pd_4M_2-a), and O(Pd_4M_2-b) in Fig. 1]. The difference of these energies represents the increment of the absorption energy (Tables 1 and 2 and Fig. 2). The linear fit of the dependence of this increment on n with $n \leq 2$ for each M (Fig. 2) yields the corresponding average H–M interaction, ϵ_{HM} (Table 3). In all the cases, this interaction is found to be positive (repulsive). Quantitatively, the interaction is relatively strong for Ta, Pt, and Au and weak for Cu. In our present statistical calculations of the absorption isotherms, this interaction was used for n up to 6. (In fact, as already noticed below Eq. (1), the contribution of sites with $n > 2$ to the absorption isotherms is nearly negligible.)

Table 1
Results of the DFT calculations: E_{site} is the total energy of a unit cell corresponding to an absorption site without hydrogen; E_{abs} and E_{abs}^* are the H absorption energies without and with the ZPE correction, respectively.

Site	E_{site} (eV)	E_{abs} (eV)	E_{abs}^* (eV)
O(Pd_6)	−559.945	−0.100	−0.178
O(Pd_5Au_1)	−558.160	−0.001	−0.031
O(Pd_4Au_2-a)	−556.386	0.217	0.188
O(Pd_4Au_2-b)	−556.354	0.050	0.079
O(Pd_5Pt_1)	−560.914	−0.001	−0.081
O(Pd_4Pt_2-a)	−561.871	0.075	0.025
O(Pd_4Pt_2-b)	−561.874	0.095	0.037
O(Pd_5Cu_1)	−558.711	−0.083	−0.139
O(Pd_4Cu_2-a)	−557.486	−0.054	−0.111
O(Pd_4Cu_2-b)	−557.460	−0.067	−0.101
O(Pd_5Ag_1)	−557.590	−0.063	−0.116
O(Pd_4Ag_2-a)	−555.236	0.072	0.051
O(Pd_4Ag_2-b)	−555.254	−0.039	−0.026
O(Pd_5Mg_1)	−558.430	−0.060	−0.109
O(Pd_4Mg_2-a)	−556.885	0.079	0.032
O(Pd_4Mg_2-b)	−556.678	−0.059	−0.062
O(Pd_5Ta_1)	−569.558	0.081	0.045
O(Pd_4Ta_2-a)	−579.106	0.388	0.370
O(Pd_4Ta_2-b)	−578.634	0.189	0.187

Table 2
Increments of the energy (in eV) of absorption of a hydrogen atom the O(Pd_5M), O(Pd_4M_2-a) and O(Pd_4M_2-b) sites compared to the absorption energy, −0.178 eV, in pure Pd [O(Pd_6)]. These data, obtained by using those presented in Table 1 (with the ZPE) correction, were employed to construct Fig. 2. The linear fit of the dependence of these increments on the number of M atoms (Fig. 2) yields ϵ_{HM} (in eV).

M	O (Pd_5M_1)	O (Pd_4M_2-a)	O (Pd_4M_2-b)	ϵ_{HM}
Mg	0.069	0.210	0.116	0.077
Cu	0.039	0.067	0.077	0.035
Ag	0.062	0.229	0.152	0.089
Ta	0.223	0.548	0.365	0.223
Pt	0.097	0.203	0.215	0.105
Au	0.147	0.366	0.256	0.150

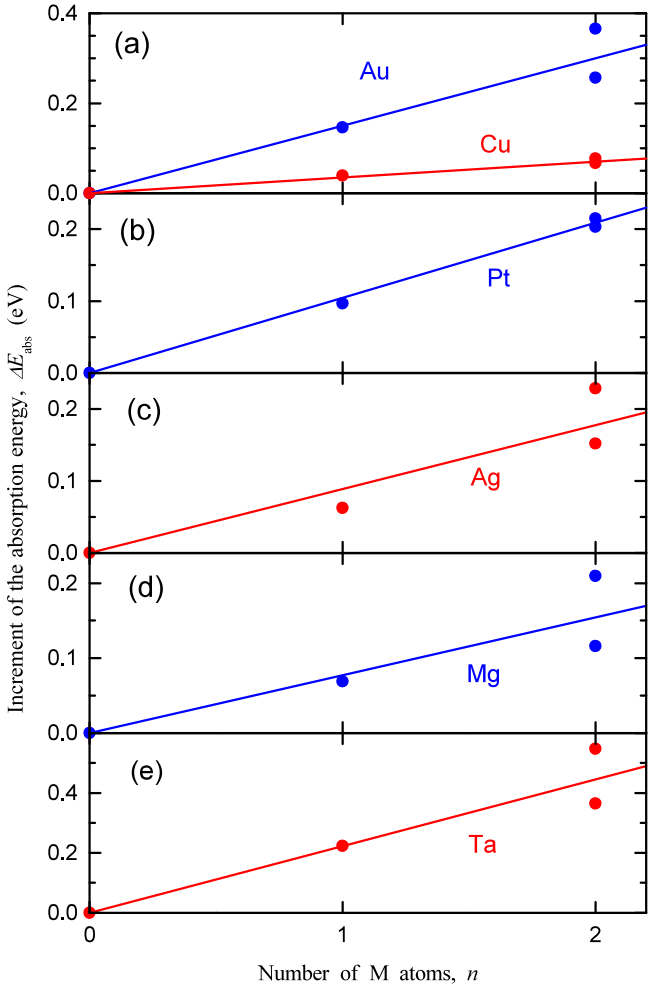

Fig. 2. Increment of the energy (with the ZPE correction) of absorption of an H atom in an O site as a function of the number of M atoms forming a site (according to the data presented in Table 1). The general trend in the dependence is linear (straight line). The corresponding slope determines ϵ_{HM}.

Table 3
The H-M interaction, ϵ_{HM}, and effective M-M interaction, ϵ_*, in binary alloys of Pd with the metals under consideration according to the DFT calculations with the ZPE corrections. The H–Au interaction presented is the same as that reported earlier [22].

M	ϵ_{HM} (eV)	ϵ_* (eV)
Mg	0.077	0.207
Cu	0.035	0.026
Ag	0.089	-0.017
Ta	0.223	0.472
Pt	0.105	-0.003
Au	0.150	0.032

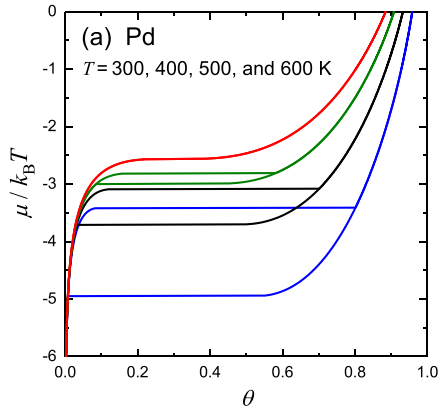

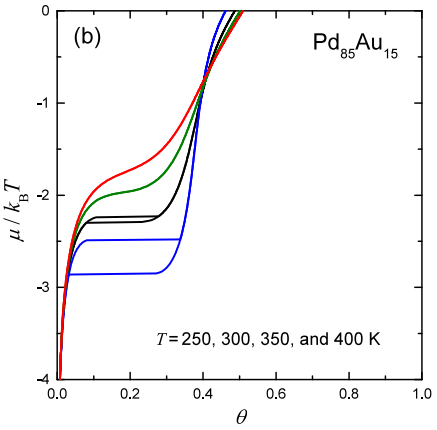

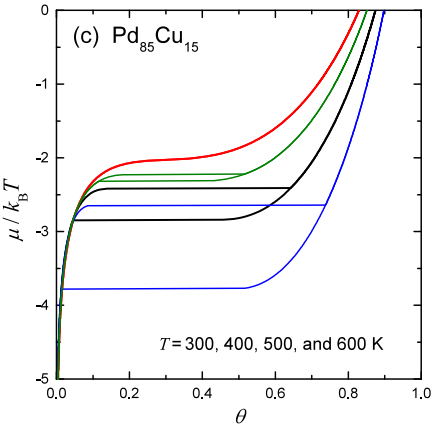

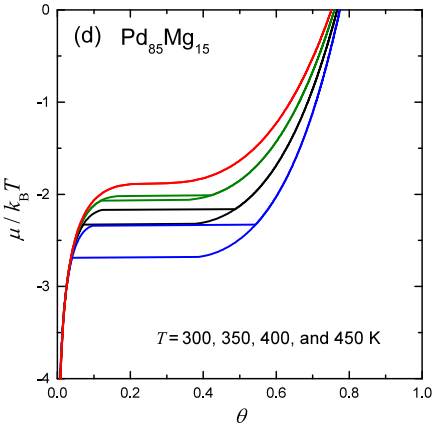

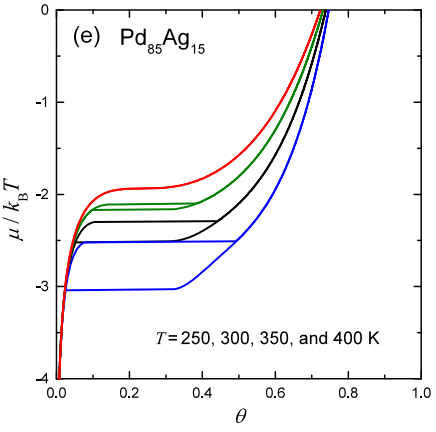

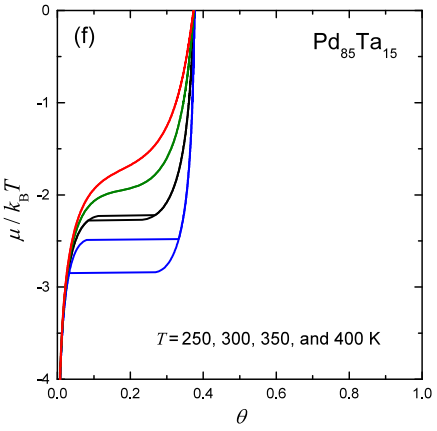

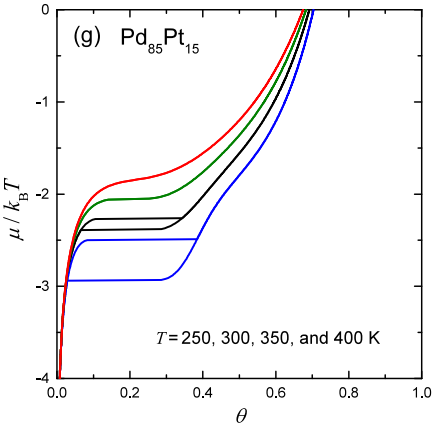

(caption on next page)

Fig. 3. Hydrogen absorption isotherms calculated according to Eqs. (1)–(5) for (a) pure Pd and alloys of Pd with (b) Au, (c) Cu, (d) Mg, (e) Ag, (f) Ta, and (g) Pt. Each panel shows isotherms at four temperatures below and slightly above T_c (the increase of temperature is marked by blue, black, olive, and red colors, respectively). In all the alloys, the fraction of Pd atoms replaced by atoms of the second metal is 0.15. The atoms in alloys are considered to be located at random (Eq. (5)). The values of the H-M interactions, ϵ_{HM}, used in the calculations are given in Table 3. (The results presented for pure Pd and a Pd–Au alloy are similar to those reported earlier [22].)

Although in general the metal-metal interaction in alloys is complex [36], some general trends can often be understood by introducing the simplest pairwise interactions, ϵ_{AA}, ϵ_{BB}, and ϵ_{AB} (A an B represent two metals; see Appendix). In the bulk, the number of bonds formed by each metal atom is constant (12 in our case), and the change of the energy related to the replacement of A by B is well known to depend on the effective interaction, $\epsilon^* = \epsilon_{AA} + \epsilon_{BB} - 2\epsilon_{AB}$, associated with the number of B-B (or A-A) pairs. This energy can be used in calculations of the total energy or chemical potential in the Bethe-Peierls approximation (see Appendix). In our context, this approach is reasonable because we are interested in the situations when f is low, and in this limit the role of the non-linear corrections in the metal-metal interaction is not central. Following this way, we can identify ϵ^* with the difference of the energies of the O(Pd_4M_2-b), and O(Pd_4M_2-a) structures (Fig. 1) in the absence of an H atom, because this difference correspond to the formation of one additional M-M bond. The corresponding values obtained by employing our DFT calculations are given in Table 3. This interaction is positive (repulsion) and appreciable in the case of Mg (ϵ^* = 0.207 eV) and Ta (ϵ^* = 0.472 eV). For Au and Cu, the interaction is 0.032 and 0.026 eV, respectively. For comparison, we can notice that for Au this interaction was earlier calculated by using DFT and taking various configurations into account [49]. The corresponding value, 0.021 eV, is somewhat lower than that obtained in our estimates based on one configuration. For Ag, the interaction is negative (attraction), − 0.017 eV. For Pt, the interaction is negative as well but nearly negligible, − 0.003 eV.

3.2. Absorption isotherms and critical temperature

Our analysis is primarily aimed at relatively large alloyed Pd-M NPs fabricated by hole-mask colloidal lithography. In such NPs with relatively small fraction of M, the arrangement of metal atoms is usually close to random [12,13]. The low values of the effective M-M interaction for the metals under consideration (Table 3; except Mg and Ta) are also if favour of nearly random alloy. For this reason, the bulk of our calculations of hydrogen absorption isotherms (Fig. 3) are based on the random-alloy approximation (Eq. (5)). As in the available experiments related to potential applications for hydrogen sensors [12,13], f is considered to be relatively low and set to 0.15. For comparison with what was already obtained and discussed earlier [22], we first present typical results for pure Pd and a Pd-Au alloy (Fig. 3(a,b)) and then similar results for alloys of Pd with Cu, Mg, Ag, Ta, or Pt (Fig. 3(c-g)).

In pure Pd (Fig. 3(a)), hydrogen is absorbed at room temperature up to the H/Pd ratio $\simeq$ 0.66 with an appreciable hysteresis. With increasing temperature, the hysteresis disappears at $T = T_c$ = 600 K.

In the alloys, the hysteresis loops are shifted to the left (Fig. 3), and T_c for the hydride formation is reduced. For f = 0.15 (Fig. 3), T_c is predicted to decrease down to $\simeq$ 330 K (Au), 550 K (Cu), 450 K (Mg), 400 K (Ag), 320 K (Ta), and 350 K (Pt). Concerning the dependence of T_c on f, we notice that at $f \lesssim 0.15$, T_c decreases nearly linearly with increasing f as was earlier already shown in the case of the Pd–Au alloy [22].

The features described above are especially appreciable in the cases of the Pd–Au and Pd–Ta alloys (Fig. 3(b,f)). The key factor behind them is that the H absorption in the O sites containing Au or Ta atoms is energetically not favourable. For this reason, the phase transition is related primarily to absorption in the sites formed only by Pd. With increasing Au or Ta amount, the fraction of such sites rapidly decreases, the distance between H atoms located there becomes on average larger, the interaction between them becomes weaker, and accordingly the driving force for the phase transition decreases.

In the Pd–Cu alloy, the H–M interaction is predicted to be weak, ϵ_{HM} = 0.035 eV (Table 3; cf. this value with the values for other metals), and accordingly the effect of the addition of Cu to Pd on the hydride formation is weak as well (Fig. 3(c)).

For the other alloys under consideration (Pd with Mg, Ag, or Pt), the H–M interaction is stronger than in the Pd–Cu case, and the situation is closer to that for the Pd–Au or Pd–Ta alloys, i.e., the effect of the addition of the second metal to Pd on the hydride formation is appreciable (cf. Figs. 3(b,f) and (d,e,g)).

Although in the systems discussed the random-alloy approximation is reasonable, the short-range correlations in the arrangement of metal atoms are in fact inevitable. In the corresponding experiments (e.g., [12,13]), the Pd–M NPs are fabricated before hydrogen absorption, the absorption occurs at relatively low temperatures, and accordingly the structure of NPs is expected to be close to that just after their fabrication. This means that the short-range correlations can be described at the level of an alloy without hydrogen. It can be done in the framework of the Bethe-Peierls approximation (Appendix) by using the already introduced metal-metal interaction, ϵ^* (Table 3). The positive value of this interaction is in favour of mixing Pd and M, whereas the negative value promotes segregation of Pd and M.

To illustrate the scale of the effect of short-range correlations in the arrangement of metal atoms on the hydrogen absorption, we focus on the Pd-Au alloy and, taking into account that in this case the scale of ϵ^* is 0.02–0.03 eV (Ref. [49] and Table 3), use ϵ^* = 0.02 eV in calculations of P_n. The corresponding absorption isotherms become narrower and are shifted to the left (Fig. 4(a)). The critical temperature for the hydride formation is reduced. These effects are well visible but not dramatic. Physically, these features are related to mixing Pd and M. It reduces slightly the number of M–M contacts and accordingly reduces also the number of the O sites formed only by Pd atoms. The latter results in the shift of the absorption isotherms to the left, because such sites are the most important for absorption.

From the tutorial point of view, it is instructive to show what happens if the repulsive interaction, ϵ^* = 0.02 eV (Fig. 4(a)), is replaced by the attractive interaction, ϵ^* = − 0.02 eV. In the later case, the absorption isotherms are wider and slightly shifted to the right (Fig. 4(b)), and the critical temperature for the hydride formation becomes higher. These features are related to the tendency of Pd and M atoms with the prescribed interaction, $\epsilon^* < 0$, to segregation.

In the examples shown in Fig. 4(a,b), ϵ^* is rather small. According to our DFT calculations, this interaction should be much larger, ϵ^* = 0.472 eV, in the Pd–Ta alloy. If this interaction is neglected, our calculations predicts hysteresis in hydrogen absorption at T = 30 °C provided $f \lesssim 0.15$ (see, e.g., Fig. 3(f)). If we take this interaction into account, the hysteresis is predicted if f is smaller than $\simeq$ 0.10 (Fig. 5). The latter is in good agrement with the experiments showing hysteresis at T = 30 °C in hydrogen absorption by a Pd–Ta film (with a thickness of 60 nm at fused silica) provided $f \lesssim 0.08$ (Fig. 6 in Ref. [17]). (Hydrogen absorption in such nanofilms with appreciable fraction of Ta has recently been studied in the context of hydrogen sensors in Ref. [50].)

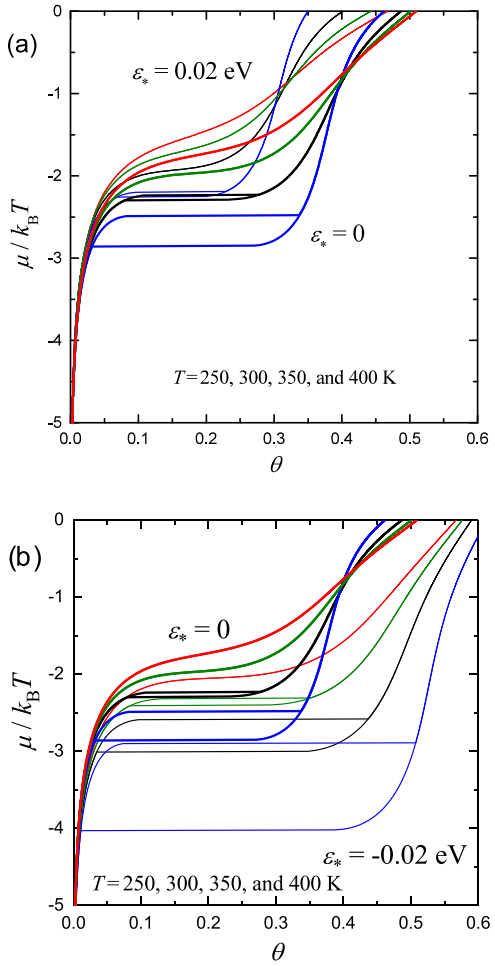

Fig. 4. (a) Hydrogen absorption isotherms calculated according to Eqs. (1)-(4) for the Pd–Au alloy with $f = 0.15$. The thick lines correspond to the random-alloy approximation (Eq. (5)). The thin lines show the results obtained by using the Bethe-Peierls approximation with $\epsilon_* = 0.02$ eV. (b) For comparison, the isotherms have been calculated also with $\epsilon_* = -0.02$ eV.

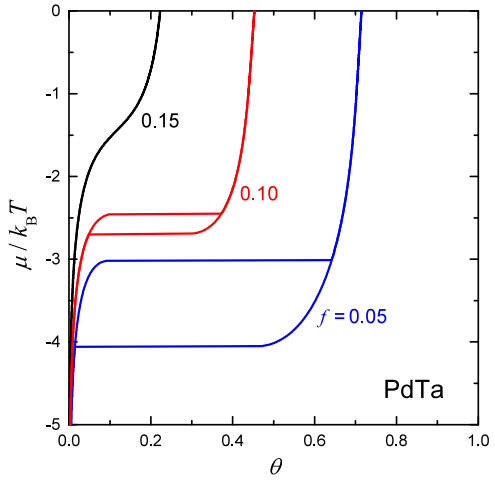

Fig. 5. Hydrogen absorption isotherms calculated for the Pd–Ta alloy at $T = 30$ °C with $\epsilon_* = 0.472$ eV and $f = 0.05$, 0.10, and 0.15.

4. Conclusion

Using the statistical models with the parameters validated by DFT, we have analyzed theoretically absorption of hydrogen in binary alloys of Pd with a small fraction of Mg, Cu, Ag, Ta, Pt, or Au. The appreciable suppression of hysteresis and decrease of the critical temperature for the hydride formation are predicted for all these additives except Cu. The bulk of the results was obtained by employing the random-alloy approximation for the arrangement of metal atoms.

The effect of the short-range correlations in the arrangement of metal atoms on the hydrogen absorption isotherms has been scrutinised as well. The tendency of metals to mixing is found to be in favour of additional suppression of hysteresis whereas the tendency to segregation makes the hysteresis loops wider. The corresponding changes in the absorption isotherms are predicted to be visible but not dramatic.

The predicted general trend in suppression of hysteresis and decrease of the critical temperature for the hydride formation is in good agreement with the available experiments for the Pd–Au NPs [12] and Pd–Ta thin films [17] (these systems have been analyzed here theoretically; the Pd–Au system was analyzed earlier as well [22]) and Pd-Ni thin films [16] (this system has not been analyzed here).

In fact, the experimental data for the Pd–Cu NPs are of the same category [13]. Our calculations predict, however, a weaker effect of Cu on the hydrogen absorption in the Pd–Cu case. The explanation why the latter is the case is not simple and this aspect merits additional studies. One of the likely reasons of the difference is that as it has been articulated in the motivation of our present study the H–M interactions are rather small in general and in the Cu case in particular, and we cannot exclude that the accuracy of DFT is not sufficient in the latter case. In principle, the reduction of the H–H interaction due to the Cu-related compression of the lattice cannot be excluded either.

Taken together, our results contribute to the formation of the theoretical basis for the interpretation of the experimental measurements of hydrogen adsorption by metal alloys. Nowadays, such experiments are numerous (see e.g. the references in [3,21]) and, as a rule, fully empirical.

CRediT authorship contribution statement

The paper was conceived and written by both authors. The DFT and statistical calculations were performed by M.M. and V.P.Zh., respectively.

Declaration of Competing Interest

The authors declare that they have no known competing financial interests or personal relationships that could have appeared to influence the work reported in this paper.

Acknowledgments

The DFT part of this work was made by M.M. at Boreskov Institute of Catalysis and supported by the Russian Science Foundation (Grant 20-43-05002). The statistical part was made by V.P.Zh. and supported by Ministry of Science and Higher Education of the Russian Federation in the framework of the budget project for Boreskov Institute of Catalysis (Grant 0239-2021-0011). This work has been carried out using facilities of Siberian Supercomputer Center of the Siberian Branch of Russian Academy of Sciences (SB RAS) and computing resources of the federal collective usage center Complex for Simulation and Data Processing for Mega-science Facilities at NRC Kurchatov Institute, http://ckp.nrcki.ru.

Appendix

Let us consider the lattice-gas model with the nearest-neighbour pairwise interactions, ϵ_{AA}, ϵ_{BB}, and ϵ_{AB}, between particles of two types, A and B (Pd and M in our present context). If an A particle interacts with m A particles and n B particles, its energy is $E_A = m\epsilon_{AA} + n\epsilon_{AB}$. If this particle is replaced by a B particle, the energy of the latter particle will be $E_B = m\epsilon_{AB} + n\epsilon_{BB}$. The increment of the energy corresponding to this replacement is equal to the difference of these energies,

$$\Delta E = E_B - E_A = m(\epsilon_{AB} - \epsilon_{AA}) + n(\epsilon_{BB} - \epsilon_{AB}). \tag{6}$$

Using the relation $m + n = n_{max}$ (n_{max} is the maximum number of bonds), one can replace n by m or m by n and rewrite Eq. (6) in terms m or n,

$$\Delta E = m(2\epsilon_{AB} - \epsilon_{AA} - \epsilon_{BB}) + n_{max}(\epsilon_{BB} - \epsilon_{AB}), \quad \text{or} \tag{7}$$

$$\Delta E = n(\epsilon_{AA} + \epsilon_{BB} - 2\epsilon_{AB}) + n_{max}(\epsilon_{AB} - \epsilon_{AA}). \tag{8}$$

The terms $n_{max}(\epsilon_{BB} - \epsilon_{AB})$ (in Eq. (7)) or $n_{max}(\epsilon_{AB} - \epsilon_{AA})$ (in Eq. (8)) are independent of m and n and can be included in statistical calculations into the baseline value for the energy or into the A or B chemical potentials. Thus, the total energy can in fact be calculated by using the number of A-B pairs and operating by the effective energy defined as $\epsilon_* = 2\epsilon_{AB} - \epsilon_{AA} - \epsilon_{BB}$ or by employing the number of B-B pairs and operating by the effective energy defined as $\epsilon_* = \epsilon_{AA} + \epsilon_{BB} - 2\epsilon_{AB}$. Except the sign, these two effective energies are equal.

In our case, A and B particles can be identified with Pd and M atoms, and the effective pairwise interaction is represented as $\epsilon_* = \epsilon_{PdPd} + \epsilon_{MM} - 2\epsilon_{PdM}$. Then, by analogy with the conventional quasi-chemical approximation, the Bethe-Peierls approximation can be used to describe short-range correlations in the arrangement of metal atoms [52]. In the latter approximation, the atoms are located in a properly chosen cluster of sites and described exactly by using the grand canonical distribution. Their interaction with the atoms located outside this cluster is taken into account by introducing the corresponding effective interaction.

In our analysis, we are interested in the arrangement of metal atoms forming an octahedral (O) site (Fig. 1) or, more specifically, in the probability, P_n, that this site is formed with participation of n M atoms ($0 \le n \le 6$). For this reason, we chose an O site as a suitable cluster for the Bethe-Peierls approximation. In the corresponding experiments, the Pd-M NPs are fabricated before hydrogen absorption, the absorption occurs at relatively low temperatures, and accordingly the structure of NPs is expected to be close to that just after their fabrication. This means that there is no need to describe the effect of hydrogen on the probabilities of interest.

To describe the distribution of Pd and M atoms in the O site, we introduce the effective chemical potential, μ, corresponding to replacement of a Pd atom by a M atom. With respect the interaction with the atoms located outside the O site, all the Pd atoms located inside the site are equivalent. The situation with M atoms is similar. This means that we can include the interaction with the atoms located outside the O site into the chemical potential and do not introduce it explicitly.

With the specification above, the partition functions, S_n, corresponding to n from 0 to 6, are defined as

$$S_0 = 1,$$
$$S_1 = 6\exp(\mu/k_BT),$$
$$S_2 = 3\exp(2\mu/k_BT) + 12\exp[(2\mu - \epsilon_*)/k_BT],$$
$$S_3 = 12\exp[(3\mu - 2\epsilon_*)/k_BT] + 8\exp[(3\mu - 3\epsilon_*)/k_BT],$$
$$S_4 = 3\exp[(4\mu - 4\epsilon_*)/k_BT] + 12\exp[(4\mu - 5\epsilon_*)/k_BT],$$
$$S_5 = 6\exp[(5\mu - 8\epsilon_*)/k_BT],$$
$$S_6 = \exp[(6\mu - 12\epsilon_*)/k_BT].$$

According to the grand canonical distribution, P_n and f are expressed via S_n as

$$P_n = S_n \Big/ \sum_{n=0}^{6} S_n, \tag{9}$$

$$f = \sum_{n=1}^{6} nP_n/6 = \sum_{n=1}^{6} nS_n \Big/ 6\sum_{n=0}^{6} S_n. \tag{10}$$

The latter equation allows us to calculate f as a function of μ or μ as a function of f. Then, using the former equation, P_n can be calculated as a function of f.

References

[1] R. Kirchheim, A. Pundt, Hydrogen in metals, in: D.E. Laughlin, K. Hono (Eds.), Physical Metallurgy, Elsevier, 2014, pp. 2597–2705.
[2] Hydrogen to the rescue. Nat. Mater. 17 (2018) 565.
[3] A. Schneemann, et al., Nanostructured metal hydrides for hydrogen storage, Chem. Rev. 118 (2018) 10775–10839.
[4] S. Dekura, H. Kobayashi, K. Kusada, H. Kitagawa, Hydrogen in palladium and storage properties of related nanomaterials: size, shape, alloying, and metal-organic framework coating effects, ChemPhysChem 20 (2019) 1158–1176.
[5] B.C. Wood, T.W. Heo, S.Y. Kang, L.F. Wan, S. Li, Beyond idealized models of nanoscale metal hydrides for hydrogen storage, Ind. Eng. Chem. Res. 59 (2020) 5786–5796.
[6] L.J. Bannenberg, C. Boelsma, K. Asano, H. Schreuders, B. Dam, Metal hydride based optical hydrogen sensors, J. Phys. Soc. Jpn. 89 (2020) 051003.
[7] I. Darmadi, F.A.A. Nugroho, C. Langhammer, High-performance nanostructured palladium-based hydrogen sensors-current limitations and strategies for their mitigation, ACS Sens. 5 (2020) 3306–3327.
[8] W.-T. Koo, et al., Chemiresistive hydrogen sensors: fundamentals, recent advances, and challenges, ACS Nano 14 (2020) 14284–14322.
[9] E. Billeter, J. Terreni, A. Borgschulte, Hydride formation diminishes CO_2 reduction rate on palladium, ChemPhysChem 20 (2019) 1398–1403.
[10] S.F. Parker, et al., The effect of particle size, morphology and support on the formation of palladium hydride in commercial catalysts, Chem. Sci. 10 (2019) 480–489.
[11] L. Chen, J.W. Medlin, H. Grönbeck, On the reaction mechanism of direct H_2O_2 formation over Pd catalysts, ACS Catal. 11 (2021) 2735–2745.
[12] F.A.A. Nugroho, I. Darmadi, V.P. Zhdanov, C. Langhammer, Universal scaling and design rules of hydrogen-induced optical properties in Pd and Pd-alloy nanoparticles, ACS Nano 12 (2018) 9903–9912.
[13] I. Darmadi, F.A.A. Nugroho, S. Kadkhodazadeh, J.B. Wagner, C. Langhammer, Rationally designed PdAuCu ternary alloy nanoparticles for intrinsically

deactivation-resistant ultrafast plasmonic hydrogen sensing, ACS Sens. 4 (2019) 1424–1432.
[14] F.A.A. Nugroho, et al., Metalpolymer hybrid nanomaterials for plasmonic ultrafast hydrogen detection, Nat. Mater. 18 (2019) 489–495.
[15] T. Gong, et al., Emergent opportunities with metallic alloys: from material design to optical devices, Adv. Opt. Mater. (2020) 2001082.
[16] E. Lee, et al., Hydrogen gas sensing performance of Pd-Ni alloy thin films, Thin Solid Films 519 (2010) 880–884.
[17] R.J. Westerwaal, et al., Thin film based sensors for a continuous monitoring of hydrogen concentrations, Sens. Actuators B 165 (2012) 88–96.
[18] M.T. Pham, et al., $Pd_{80}Co_{20}$ nanohole arrays coated with poly(methyl methacrylate) for high-speed hydrogen sensing with a part-per-billion detection limit, ACS Appl. Nano Mater. 4 (2021) 3664–3674.
[19] Y. Imry, S. Ma, Random-field instability of the ordered state of continuous symmetry, Phys. Rev. Lett. 35 (1975) 1399–1401.
[20] H. Hemmes, E. Salomons, R. Griessen, P. Sänger, A. Driessen, Lattice-gas model for the formation of palladium-silver hydrides at pressures up to 100 GPa, Phys. Rev. B 39 (1989) 10606–10613.
[21] V.P. Zhdanov, A generic statistical model of hydride formation in a random alloy, Mod. Phys. Lett. B 30 (2016) 1650330.
[22] M. Mamatkulov, V.P. Zhdanov, Suppression of hysteresis in absorption of hydrogen by a Pd–Au alloy, Phys. Rev. E 101 (2020) 042130.
[23] K. Reuter, M. Scheffler, First-principles atomistic thermodynamics for oxidation catalysis: surface phase diagrams and catalytically interesting regions, Phys. Rev. Lett. 90 (2003) 046103.
[24] K. Reuter, Ab initio thermodynamics and first-principles microkinetics for surface catalysis, in: J. Frenken, I. Groot (Eds.), Operando Research in Heterogeneous Catalysis, 114 Springer Series in Chemical Physics, 2017, pp. 541–563.
[25] J.M. Rahm, J. Löfgren, E. Fransson, P. Erhart, A tale of two phase diagrams: interplay of ordering andhydrogen uptake in Pd-Au-H, Acta Mater. 211 (2021) 116893.
[26] J.K. Nørskov, T. Bligaard, J. Rossmeisl, C.H. Christensen, Towards the computational design of solid catalysts, Nat. Chem. 1 (2009) 37–46.
[27] M. Anand, B. Rohr, M.J. Statt, J.K. Nørskov, Scaling relationships and volcano lots in homogeneous catalysis, J. Phys. Chem. Lett. 11 (2020) 8518–8526.
[28] S.S. Setayandeh, C.J. Webb, E.M. Gray, Electron and phonon band structures of palladium and palladium hydride: a review, Progress Solid State Chem. 60 (2020) 100285.
[29] S.S. Setayandeh, T. Gould, A. Vaez, E.M. Gray, Effect of pseudopotential choice on the calculated electron and phonon band structures of palladium hydride and its vacancy defect phases, Intern. J. Hydr. Energy 6 (2021) 943–954.
[30] S.S. Setayandeh, T. Gould, A. Vaez, K. McLennan, N. Armanet, E.M. Gray, First-principles study of the atomic volume of hydrogen in palladium, J. Alloys Compd. 864 (2021) 158713.
[31] A. Borgschulte, et al., Inelastic neutron scattering evidence for anomalous H–H distances in metal hydrides, Proc. Natl. Acad. Sci. USA 117 (2020) 4021–4026.
[32] B.W.J. Chen, M. Mavrikakis, Effects of composition and morphology on the hydrogen storage properties of transition metal hydrides: insights from PtPd nanoclusters, Nano Energy 63 (2019) 103858.
[33] L. Chen, Q. Wang, W. Jiang, H. Gong, Hydrogen solubility in Pd_3Ag phases from first-principles calculation, Metals 9 (2019) 121.
[34] X. Zhou, W.A. Curtin, First principles study of the effect of hydrogen in austenitic stainless steels and high entropy alloys, Acta Mater. 200 (2020) 932–942.
[35] I.A. Troyan, et al., Anomalous high-temperature superconductivity in YH_6, Adv. Mater. (2021) 2006832.
[36] R. Ferrando, J. Jellinek, R.L. Johnston, Nanoalloys: from theory to applications of alloy clusters and nanoparticles, Chem. Rev. 108 (2008) 845–910.
[37] R.B. Schwarz, A.G. Khachaturyan, (a) Thermodynamics of open two-phase systems with coherent interfaces, Phys. Rev. Lett. 74 (1995) 2523–2526;
(b) Thermodynamics of open two-phase systems with coherent interfaces: Application to metal-hydrogen systems. Acta Mater. 54 (2006) 313–323.
[38] H.C. Jamieson, G.C. Weatherly, F.D. Manchester, The $\beta \rightarrow \alpha$ phase transformation in palladium-hydrogen alloys, J. Less Common. Met. 50 (1976) 85–102.
[39] P.J. Cappillino, E.J. Lavernia, M.D. Ong, W.G. Wolfer, N.Y. Yang, Plastic deformation and hysteresis for hydrogen storage in Pd–Rh alloys, J. Alloys Compd. 586 (2014) 59–65.
[40] A. Baldi, T.C. Narayan, A.L. Koh, J.A. Dionne, *In situ* detection of hydrogen-induced phase transitions in individual palladium nanocrystals, Nat. Mater. 3 (2014) 1143–1148, Sec. 3 in Suppl. Inform.
[41] S. Syrenova, et al., Hydride formation thermodynamics and hysteresis in individual Pd nanocrystals with different size and shape, Nat. Mater. 14 (2015) 1236–1244, Sec. 7.4 in Suppl. Inform.
[42] R. Griessen, N. Strohfeldt, H. Giessen, Thermodynamics of the hybrid interaction of hydrogen with palladium nanoparticles, Nat. Mater. 15 (2016) 311–317.
[43] R.B. Schwarz, A.K. Khachaturyan, A. Caro, M.I. Baskes, E. Martinez, Coherent phase decomposition in the Pd–H system, J. Mater. Sci. 55 (2020) 4864–4882.
[44] G. Kresse, J. Hafner, *Ab initio* molecular-dynamics simulation of the liquid-metal-amorphous-semiconductor transition in germanium, Phys. Rev. B 49 (1994) 14251–14269.
[45] G. Kresse, J. Furthmüller, Efficient iterative schemes for ab initio total-energy calculations using a plane-wave basis set, Phys. Rev. B 54 (1996) 11169–11186.
[46] H. Kimizuka, S. Ogata, M. Shiga, Mechanism of fast lattice diffusion of hydrogen in palladium: interplay of quantum fluctuations and lattice strain, Phys. Rev. B 97 (2018) 014102.
[47] M.P. Belov, A.B. Syzdykova, Yu.Kh. Vekilov, I.A. Abrikosov, Hydrogen in palladium: anharmonicity of lattice dynamics from first principles, Phys. Sol. State 57 (2015) 260–265.
[48] K. Lee, M. Yuan, J. Wilcox, Understanding deviations in hydrogen solubility predictions in transition metals through first-principles calculations, J. Phys. Chem. C 119 (2015) 19642–19653.
[49] G. Kovács, S.M. Kozlov, K.M. Neyman, Versatile optimization of chemical ordering in bimetallic nanoparticles, J. Phys. Chem. C 121 (2017) 10803–10808.
[50] L. Bannenberg, H. Schreuders, B. Dam, Tantalum-palladium: hysteresis-free optical hydrogen sensor over 7 orders of magnitude in pressure with sub-second response, Adv. Funct. Mater. (2021) 2010483.
[51] A. Houari, S.F. Matar, V. Eyert, Electronic structure and crystal phase stability of palladium hydrides, J. Appl. Phys. 116 (2014) 173706.
[52] V.P. Zhdanov, Elementary Physicochemical Processes on Solid Surfaces, Plenum, 1991.